Bidirectional Reflectance Measurements of Two Snow Types

S. TAYLOR[1], G.KOH[1], R.E. DAVIS[1] AND D.J. FISK[1]

ABSTRACT

Normalized reflectance measurements of snow were made at visible and near-infrared wavelengths. Measurements at 5 zenith and 14 azimuth angles were made to calculate the bidirectional reflectance distribution functions (BRDF) of different snow types. The snow density and grain size were obtained to relate the physical and spectral properties of the snow cover. The spectral measurements show significant anisotropy in the BRDF of the two snow types discussed in this paper. Implications of these results for energy budget calculations of snow covers and remote characterization of snow cover properties are discussed.

Key words: Bidirectional reflectance distribution function, Reflectance measurements, Snow characterization, Snow types

INTRODUCTION

The investigation of snow optical properties is of interest for energy budget calculations of snow covers and for extracting information about snow cover properties from remotely sensed data. A parameter of particular interest is albedo, which is the ratio of reflected energy relative to that incident on an area over the same wavelength region. Albedo is used in energy budget models of the earth's surface because it is an indication of the amount of energy not absorbed by the surface.

For global energy balance models, it would be useful to measure albedo (or a quantity that could be consistently related to the albedo of the surface) from satellites since they provide large scale, repeat coverage of an area. Satellite remote sensing systems, however, cannot measure albedo. They measure the upwelling radiance of a parcel of the Earth's surface at an angle close to the nadir (looking straight down onto the surface) and so measure only a portion of the energy being reflected from the surface.

Because the energy reflected by a snow cover is not Lambertian (diffuse) and depends upon a number of factors, such as sun angle, viewing angle, surface roughness and surface moisture, the angular distribution of the reflected energy is required to infer snow albedo from satellite data. Normalized reflectance measurements made at 5 zenith and 14 azimuth angles indicate how the reflected energy is distributed and allow us to calculate the BRDF of the snow.

Experimental investigations of snow BRDF are limited (Kuhn 1985, Steffan 1987, Dozier et al. 1988, and Nolin et. al. 1994) and the dependence of the BRDF on wavelength, snow grain size and surface irregularities has yet to be clearly established. We made a suite of normalized reflectance measurements on the same patch of snow, and then characterized the snow. By measuring a wide variety of snow types we hope to provide useful information to researchers who use remote sensing for estimating energy balance over snow-covered areas. This paper presents the results of measurements made on two snow types that showed significant anisotropic reflectance.

EXPERIMENTAL METHODS

Spectral measurements

The spectral reflectance measurements were made outdoors at the Cold Regions Research and Engineering Laboratory in Hanover, New Hampshire, using an Analytical Spectral Devices (ASD) field-portable radiometer. The radiometer has a 1-nm sampling interval and a 3-nm wavelength accuracy. The ASD acquires a spectrum from 350 to 1050 nm; however, due to low signal levels at the ends of the spectrum, we present only the results from 400 to 900 nm.

The ASD was mounted on a goniometer-like device (Fig. 1), which allowed the viewing azimuth and zenith angle to be varied over a hemisphere, and which was placed level with a clean, flat area of snow. At a zenith angle of 0° the radiometer was 50 cm above the snow surface. The reflectance was meas-

[1] U.S. Army Cold Regions Research and Engineering Laboratory (CRREL), 72 Lyme Road, Hanover, New Hampshire 03755-1290 USA

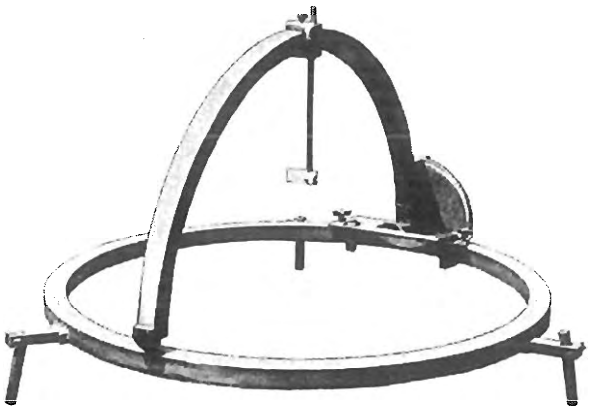

Figure 1. Goniometer-like device used to hold detector and make spectral reflectance measurements over a range of instrument azimuth and zenith angles.

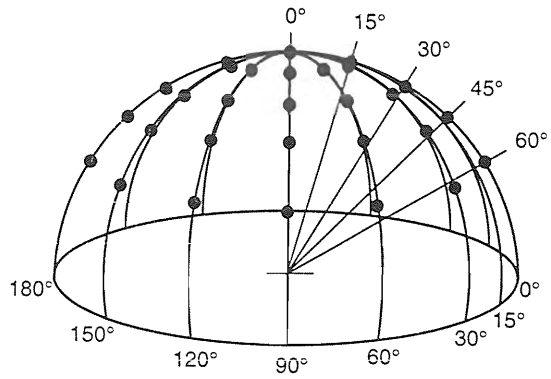

Figure 2. Reflectance measurements were made at each point on the hemisphere (only half of the measurements are shown).

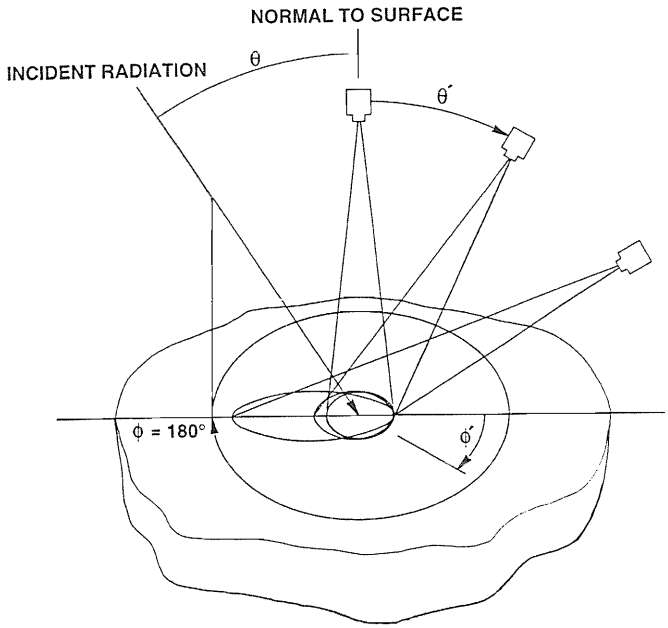

Figure 3. Ray aiagram showing the convention used for describing the measurements. The angles θ and θ′ are the solar zenith and radiometer zenith angles, ϕ is the solar azimuth and was 180° for these measurements and ϕ′ is the radiometer's azimuth. At a ϕ′ = 0 the radiometer is pointing toward the sun.

ured at 5 zenith angles at each of 14 azimuth angles (Fig. 2). At $\phi' = 0°$, the instrument was looking toward the sun (Fig. 3).

Each suite of measurements took about 30 minutes, during which time both the azimuth and zenith of the sun moved about 4°. Repeat measurements of the standard at the end of the run showed that the solar motion had only a slight effect on the spectra. A 5° foreoptic attachment gave the radiometer a 4-cm-diameter 'footprint' at $\theta' = 0°$. As θ' was increased from 0° to 15°, 30°, 45° and 60°, the area of the 'footprint' increased as $1/\cos \theta'$. Although a larger area of snow is measured at larger zenith angles, the snow properties were not thought to be different over areas of 50 to 100 cm^2. All measurements were normalized to the reflectance of a 30-cm × 30-cm Spectralon standard (98 to 99 % reflectance over the wavelengths of interest) measured at $\theta' = 0$. Each suite of measurements allows one to estimate the BRDF of a particular snow at one solar elevation.

Snow characterization

Detailed characterization of the snow is required to establish the relationship between physical and

spectral properties of the snow. The snow characterization included the snow density, snow type and grain size. The snow density was obtained gravimetrically and the snow type was classified using *The International Classification for Seasonal Snow on the Ground* (Colbeck et al. 1990). To determine the snow grain size and shape, photographs of the snow grains near the surface were obtained. These photographs were digitized and image analysis software was used to measure their projected areas and shape factors (a measure of how nearly a snow grain is circular). The measured areas were then converted to equivalent radius (radius of a circle with the same area).

Samples of the snow were collected for sectioning so that stereologic analysis and surface roughness measurements could be made on polished sections. The snow was collected in its aggregated state so as not to disturb its structure. A supercooled, liquid pore filler was used to fill the snow's pore space. After freezing the pore filler, the specimens were mounted on glass plates and planed with a sledge microtome. When left to sublimate for a few hours the planed surface develops sublimation pits in the ice but not in the pore filler. Black powder is then used to dust the surface and, as the powder fills the pits, it creates a high contrast sample from which a digital image can be made. This procedure produced two-dimensional maps of the texture of the snow and surface (e.g., Perla 1982).

RESULTS AND CONCLUSIONS

Normalized reflectance measured from two different snow types are presented. Type A snow consisted of 3 mm of surface hoar (class 7a) overlying 7 mm of bubbly ice (rain crust, class 9b), 3 mm of bonded sleet particles (class 1h), 20 mm of strongly bonded fine-grained snow (class 4a) and 40 mm of weakly bonded fine-grained snow (class 4b). Individual surface hoar particles were smaller than 1 mm, but there were chains of particles as long as 10 mm. Although it was not possible to measure the surface hoar's density in the field, we estimated that it was below 100 kg/m^3. Type B snow was collected in northern Vermont and sieved into a 15.5-cm-deep Styrofoam container. The snow was composed of broken particles (class 2b) smaller than 1 mm, with aggregates from 1 to 3 mm. The average density was 180 kg/m^3.

Photographs of the surface snow show that the type A snow particles were larger than type B snow particles (Fig. 4a and b). Image analyses done on 50 to 60 particles from each snow type revealed that the average equivalent radius was 0.7 mm for type A and 0.5 mm for type B. The shape factors were similar:

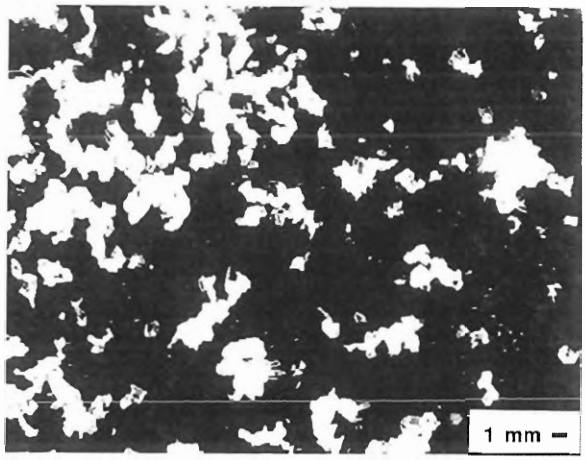

a. Type A.

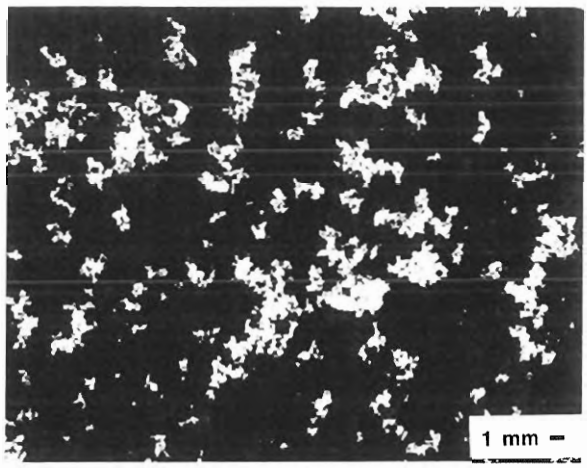

b. Type B.

Figure 4. Snow grains and aggregates of snow surfaces.

0.7 for type A, 0.65 for type B. We are still working on how to best quantify the surface roughness of the snow.

The two snow types were measured at two solar elevation angles. Figures 5 and 6 show the normalized reflectance as a function of wavelength for snow type A at viewing angle $\phi' = 0°$ and $\theta' = 0°$, 15°, 30°, 45°, and 60°. Figures 5 and 6 correspond to solar zenith angles of approximately 55° and 70°, respectively. These figures illustrate that forward scattering (anisotropic scattering from the surface of the snow cover) becomes more pronounced as the solar zenith angle increases and as the wavelength increases. Similar trends were observed in type B snow as illustrated in Figures 7 and 8.

When plots showing data taken at one zenith angle and all azimuthal angles are examined, the spectra taken at $\phi' = 0$ and 345 are the most reflective. Figure 9 illustrates this forward scatter for type A snow. Forward scattering in snow has been observed and modeled by various researchers (Nolin et al., 1994; Dozier

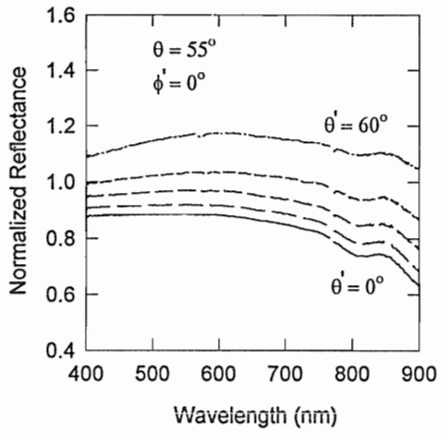

Figure 5. Spectra of type A snow at θ =55°, θ′ = 0°, 15°, 30°, 45°, 60°, and φ′ = 0°.

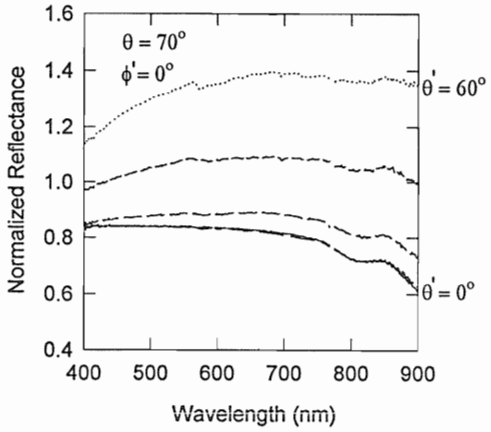

Figure 6. Spectra of type A snow at θ = 70°, θ′ = 0°, 15°, 30°, 45°, 60°, and φ′ = 0°.

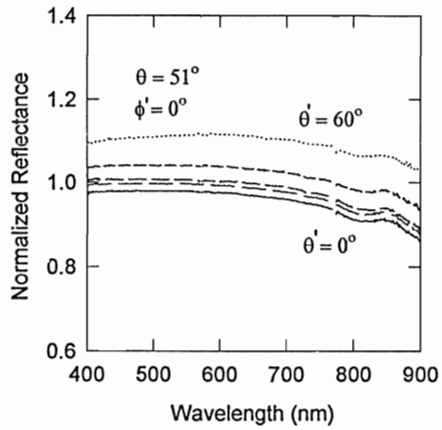

Figure 7. Spectra of type B snow at θ = 51°, θ′ = 0°, 15°, 30°, 45°, 60°, and φ′ = 0°.

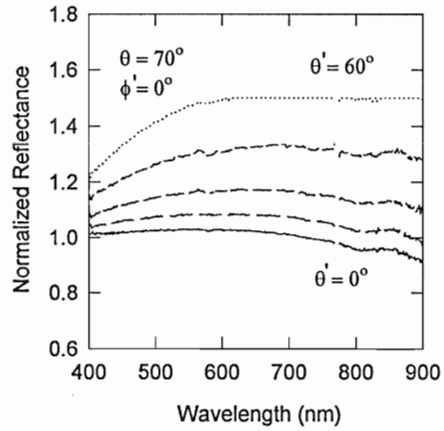

Figure 8. Spectra of type B snow at θ = 70°, θ′ = 0°, 15°, 30°, 45°, 60°, and φ′ = 0°.

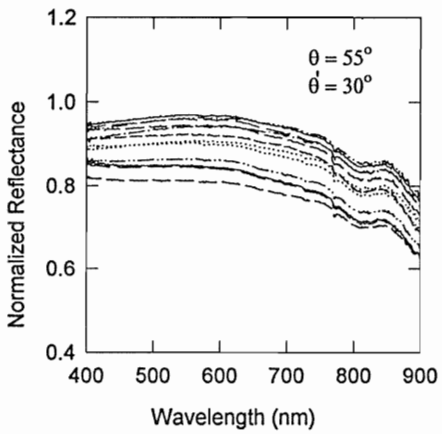

Figure 9. Reflectance spectra of type A snow taken at θ′ = 30 and all φ′. The two spectra with the highest reflectance were φ′ =0° and 345°. The spectrum with the lowest reflectance was measured at φ′ =180°.

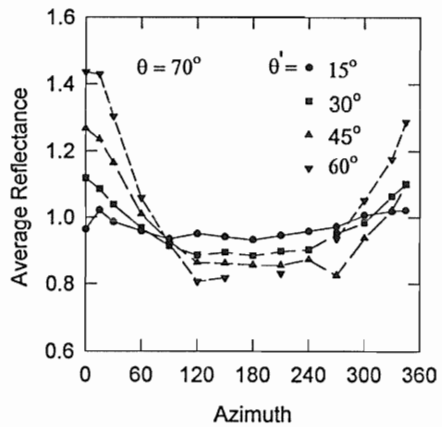

Figure 10. The reflectance values over the wavelength range 350 to 1100 nm were summed and the average value is plotted here as a function of azimuth angle. Data points not shown are low values caused by the instrument's shadow on the snow.

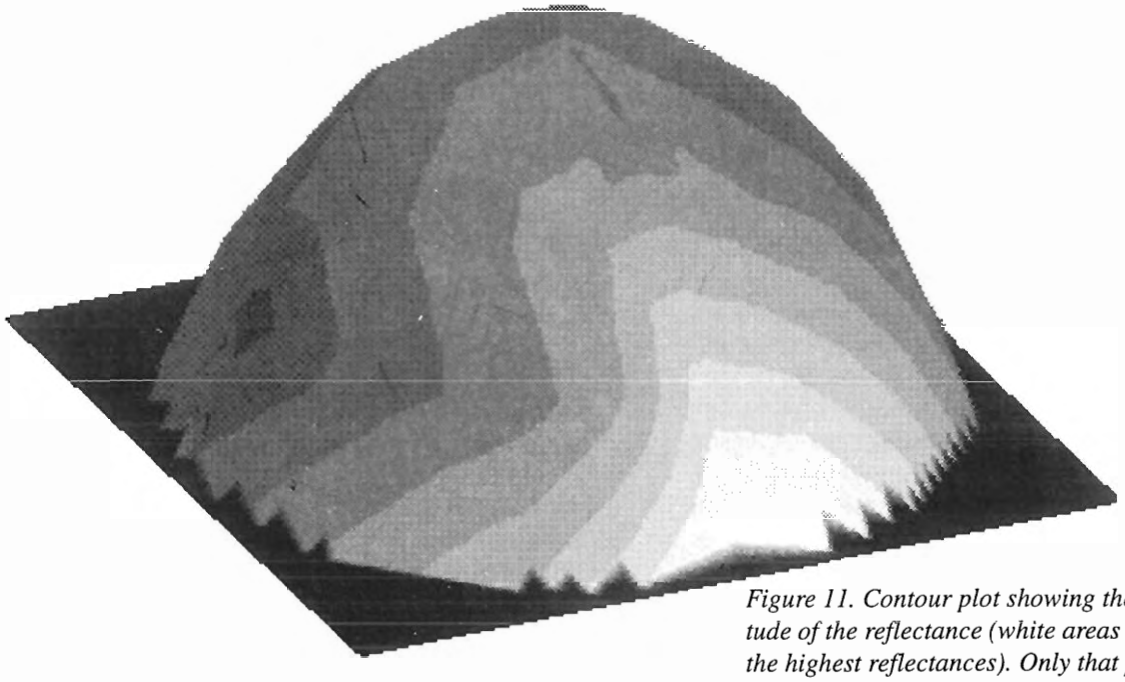

Figure 11. Contour plot showing the magnitude of the reflectance (white areas represent the highest reflectances). Only that portion of the hemisphere where data were obtained (zenith angles between 0° and 60° instead of the full 90°) is shown.

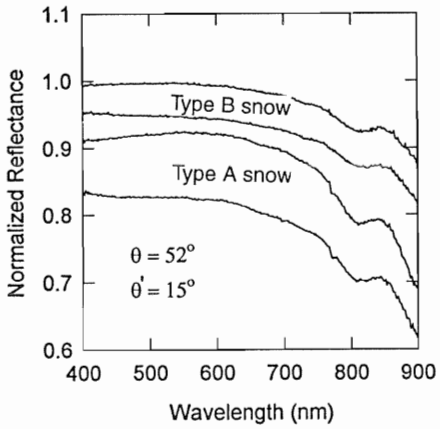

Figure 12. Reflectance spectra taken at θ′ = 15° and all ϕ′ for type A and B snow. Solar zenith angles were comparable and between 50° and 54°.

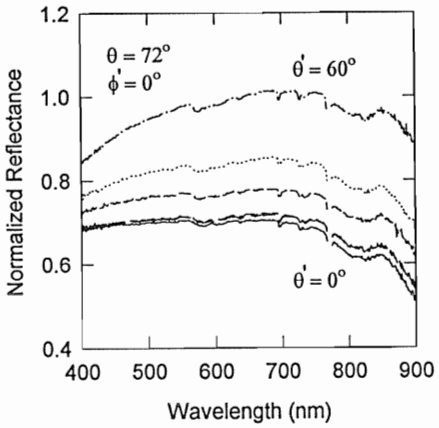

Figure 13. Spectra of ice crust underlying the type A snow. Measurements were made at θ = 72°, θ′ = 0°, 15°, 30°, 45°, 60°, and ϕ′ = 0°.

et al. 1988; Kuhn 1985, Wiscombe and Warren 1980). Figure 10 plots the average reflectance of all wavelengths versus azimuth for type B snow and clearly shows the forward scattering component. This plot shows data taken at θ = 70° at which forward scattering is higher than, but similar to, measurements made at θ = 55°.

BRDF can be visually represented as a contour plot on a hemisphere (Fig. 11) where brightness corresponds to the magnitude of the measured reflectance over the hemisphere. For the solar angles and the snow types investigated, the BRDF was characterized by strong anisotropy due to forward scattering.

There are some spectral differences between the two snow types. Type A snow has a lower spectral reflectance than the type B at comparable solar zenith angles, and is less reflective in the IR (Fig. 12). One explanation for these differences is that the measurements made of the type A snow are a mixture of the spectral characteristics of the snow and the underlying ice layer.

Spectral reflectance measurements were made of the ice underlying snow type A at $\phi' = 0$ for $\theta' = 0°$, 15°, 30°, 45°, and 60° and $\theta = 72°$ and are shown in Figure 13. The reflectance of the icy crust is lower than that of snow (0.7, compared to 0.9, for the spectra at $\theta' = 0$) and there is a pronounced decrease in the IR. The differences between the spectra of snow and those of glaze and ice have been documented by Perovich (1994).

Additional measurements on many snow types are needed to quantify the effects of snow properties on the BRDF. BRDF measurements of snow can lead to an improvement in modeling of energy balance in a snow cover. If the forward scattering contribution to the BRDFcan be established, one can estimate the amount of energy entering the snowpack. At the solar angles investigated in this work, the reflectance measurements suggest that a significant part of the incident solar radiation is reflected at the surface and does not enter the snowpack. The shape of the BRDF indicates that satellite systems, which do not measure forward or backscatter, can underestimate or overestimate the snow's albedo.

REFERENCES

Colbeck, S., E. Akitaya, R. Armstrong, H. Gubler, J. Lafeuille, K. Lied, D. McClung and E. Morris (1990) *The International Classification for Seasonal Snow on the Ground.* International Commission on Snow and Ice (ICSI). Available from World Data Center, University of Colorado, Boulder, Colorado.

Dozier, J., R.E. Davis, A.T.C. Chang and K. Brown (1988) The spectral bidirectional reflectance of snow. In *Proceedings of the 4th International Colloquium on Spectral Signatures of Objects in Remote Sensing.* European Space Agency, Special Publication 287, p. 87–92.

Grenfell, T.C. and D.K. Perovich (1981) Radiation absorption coefficients of polycrystalline ice from 400–1400 nm. *Journal of Geophysical Research*, **86**: 7447–7450.

Kuhn, M. (1985) Bidirectional reflectance of polar and alpine snow surfaces. *Annals of Glaciology,* **6**: 64–167.

Nolin, A. W., K. Steffen and J. Dozier (1994) Measurement and modeling of the bidirectional reflectance of snow. *IEEE*, p. 1919–1921.

Perla, R.I. (1982) Preparation of section planes in snow specimens. *Journal of Glaciology*, **28**(98): 199–204.

Perovich, D.K. (1994) Light reflection from sea ice during the onset of melt. *Journal of Geophysical Research*, **99**: 3351–3359.

Steffen, K. (1987) Bidirectional reflectance of snow at 500–600 nm. In Large-Scale Effects of Seasonal Snowcover. *IAHS Publications*, **166**: 415–425.

Wiscombe, W.J. and S.G. Warren (1980) A model for the spectral albedo of snow. I: Pure snow. *Journal of Atmospheric Sciences,* **37**: 2712–2733.